# Molecular Determinants and Evolutionary Dynamics of Wobble Splicing

*Jianning Lv,*[1] *Yun Yang,*[1] *Heng Yin,* Fengjiao Chu,† Haitao Wang,* Wenjing Zhang,* Yaozhou Zhang,† and Yongfeng Jin*†*

*Institute of Biochemistry, College of Life Sciences, Zhejiang University (Zijingang Campus), Hangzhou, Zhejiang, China; and †Institute of Biochemistry, College of Life Sciences, Zhejiang Sci-Tech University, Hangzhou, Zhejiang, China

Alternative splicing at tandem splice sites (wobble splicing) is widespread in many species, but the mechanisms specifying the tandem sites remain poorly understood. Here, we used *synaptotagmin I* as a model to analyze the phylogeny of wobble splicing spanning more than 300 My of insect evolution. Phylogenetic analysis indicated that the occurrence of species-specific wobble splicing was related to synonymous variation at tandem splice sites. Further mutagenesis experiments demonstrated that wobble splicing could be lost by artificially induced synonymous point mutations due to destruction of splice acceptor sites. In contrast, wobble splicing could not be correctly restored through mimicking an ancestral tandem acceptor by artificial synonymous mutation in *in vivo* splicing assays, which suggests that artificial tandem splice sites might be incompatible with normal wobble splicing. Moreover, combining comparative genomics with hybrid minigene analysis revealed that alternative splicing has evolved from the 3′ tandem donor to the 5′ tandem acceptor in *Culex pipiens*, as a result of an evolutionary shift of *cis* element sequences from 3′ to 5′ splice sites. These data collectively suggest that the selection of tandem splice sites might not simply be an accident of history but rather in large part the result of coevolution between splice site and *cis* element sequences as a basis for wobble splicing. An evolutionary model of wobble splicing is proposed.

## Introduction

Alternative splicing plays a major role in the generation of proteomic and functional diversity in metazoan organisms (Black 2003; Blencowe 2006). A subtle variation of transcripts may come from alternative splicing at the tandem splice sites in close proximity (Hiller et al. 2004; Lai et al. 2006; Tsai and Lin 2006; Hiller and Platzer 2008). This often leads to the insertion/deletion (InDel) of a single or a few amino acids while maintaining the open reading frame (Hiller et al. 2004; Lai et al. 2006; Tsai and Lin 2006; Hiller and Platzer 2008). Such wobble splicing is predicted to exist in 30% of human genes and is active in at least 5% of genes (Hiller et al. 2004). Conservation of such events points to important functions (Nakhost et al. 2003; Hiller et al. 2008). In addition, experimental studies have also revealed functional differences for tandem sites that lack deep evolutionary conservation (Condorelli et al. 1994); thus, species-specific alternative splice events at tandem sites may have functional consequences (Hiller et al. 2008). Although wobble splicing only subtly changes the protein sequence and structure (Hiller et al. 2004), it might increase the functional diversity of proteins (Condorelli et al. 1994; Englert et al. 1995; Vogan et al. 1996; Hu et al. 1999; Maugeri et al. 1999; Merediz et al. 2000; Yan et al. 2000; Joyce-Brady et al. 2001; Burgar et al. 2002; Tadokoro et al. 2005; Unoki et al. 2006; Tsai et al. 2007, 2008).

Tandem splice sites are common in human genes, and a considerable fraction of genes have been confirmed to generate wobble splicing isoforms (Englert et al. 1995; Hiller et al. 2004; Tadokoro et al. 2005; Tsai and Lin 2006). Recent reports have indicated that several features of wobble splicing differ from those of constitutive splicing, such as high conservation of the intron sequence upstream of the tandem splice site (Akerman and Mandel-Gutfreund 2006; Koren et al. 2007; Tsai et al. 2007; Hiller et al. 2008), but the mechanisms and basic determinants of tandem splicing are still poorly understood. The clue to understanding this feature requires a promising candidate with conservation over longer evolutionary distances for further experimental studies (Hiller et al. 2008). Synaptotagmin I (SytI), a $Ca^{2+}$ sensor for synchronous neurotransmitter release, generated two spliced isoforms ($SytI_{VQ}$ and SytI) in *Aplysia californica*, whereas expression of $SytI_{VQ}$, but not of SytI, blocked 5-HT-mediated reversal of depression (Nakhost et al. 2003). Here, we envisage *sytI* as a model to carry out detailed evolutionary analysis of functional wobble splicing from different insects spanning more than 300 My of evolution: *Drosophila melanogaster*, *Culex pipiens* (Diptera), *Bombyx mori* (Lepidoptera), *Tribolium castaneum* (Coleoptera), *Apis mellifera* (Hymenoptera), and *Pediculus humanus* (Phthiraptera). Comparative analysis indicated that the occurrence of species-specific wobble splicing was related to tandem splice sites. Mutagenesis experiments demonstrated that tandem splice sites are necessary but not sufficient for wobble splicing. Moreover, combining comparative genomics with mutational analysis revealed that alternative splicing has evolved from the 3′ to 5′ tandem splice site in *C. pipiens*, as the result of an evolutionary shift of *cis* element sequences from 3′ to 5′ splice sites. An evolutionary model of wobble splicing is proposed.

## Materials and Methods

### Materials

Fruit flies (*D. melanogaster*), mosquitoes (*C. pipiens*), silkworms (*B. mori*), red flour beetles (*T. castaneum*), honeybees (*A. mellifera*), and human head lice (*P. humanus*) were obtained as previously reported (Yang et al. 2008). Water fleas (*Daphnia magna*) were donated by Dr. Li Shaonan of the Institute of Pesticide and Environmental Toxicology, Zhejiang University. *Xenopus laevis* were kindly provided by the Institute of Cell and Genetics, Zhejiang University. Total RNA was isolated using the RNeasy Mini Kit (Qiagen, Hilden, Germany), according

[1] These authors contributed equally to this work.

Key words: wobble splicing, evolution, mutagenesis experiment, synonymous substitution, *sytI*.

E-mail: jinyf@zju.edu.cn.

*Mol. Biol. Evol.* 26(5):1081–1092. 2009
doi:10.1093/molbev/msp023
Advance Access publication February 12, 2009

to the manufacturer's protocol. Genomic DNA was isolated using the Universal Genomic DNA Extraction Kit (TaKaRa, Dalian,China).

### Gene Structure Analysis and Verification

Genomic DNA sequences and corresponding protein sequences of other insect *sytI* homologs were obtained through Blast searches, using the fruit fly (*D. melanogaster*) homolog sequence as bait (Perin et al. 1991). Contigs within which each homolog resides are described below: *D. melanogaster*: AABU01002692.1; *C. pipiens*: DS231887.1; *B. mori*: AADK01011502.1, AADK01020847.1; *T. castaneum*: NW_001092820.1; *A. mellifera*: NW_001253173.1, NW_001253172.1; *P. humanus*: DS235852.1; and Dma: *D. magna* (FJ550353). Other invertebrate and vertebrate *sytI* orthologs in *Homo sapiens* (human) and *Lymnaea stagnalis* (snail), among other species, were identified by Blast searches using the sequence of the most closely related organism and confirmed by available genome annotation and phylogenetic analysis (Geppert et al. 1994; Zhang et al. 1994; Craxton 2001; Nakhost et al. 2003; Craxton 2004) (supplementary fig. S1, Supplementary Material online). Potential alternative splicing sites were either verified with expressed sequence tag (EST) evidence or reverse transcriptase polymerase chain reaction (RT-PCR). Full-length cDNA clones were obtained using RT-PCR or the 5′/3′ rapid amplification of cDNA ends cDNA synthesis kit (Invitrogen, Carlsbad, CA).

### RT-PCR and Verification of Wobble Splicing

Total RNA was reverse transcribed using SuperScript III RTase (Invitrogen) with oligo$(dT)_{15}$ primer, and the resulting single-stranded cDNA product was treated with DNase I at 37 °C for 30 min. The specific primers flanking the wobble splicing site were designed according to the *sytI* sequence (table 1). RT-PCR products were gel purified and subjected to direct sequencing with corresponding specific primers. In addition, the products of RT-PCR were purified and cloned into the pGEM-T Easy vector (Promega, Madison, WI) and transformed into JM109 competent cells. Recombinant clones were identified by restriction enzyme digestion and PCR. Sequencing of individual clones was done using an automatic DNA sequencer.

### Quantification of mRNA Isoforms

The quantification of the splice form ratio was performed using RT-PCR gel electrophoresis as described by Tadokoro et al. (2005). Total RNA was isolated from different development stages and tissue samples. RT-PCR was carried out under the following cycling conditions with an initial denaturation of 2 min at 94 °C followed by 30–35 cycles of denaturation at 94 °C for 30 s, annealing at 60–65 °C for 1 min, and extension at 72 °C for 15 s, with a final extension at 72 °C for 10 min. As *sytI* expression levels in tissues varied extensively, the amount of transcribed RNA in RT-PCR was adjusted to give a similar level of PCR products to facilitate the detection of two isoforms with a 6- or 9-nt difference. Amplified PCR products were separated by electrophoresis through a 12% polyacrylamide gel and then detected by silver staining. Images were captured through a Charge Coupled Device camera, and the quantification of mRNA isoforms was done by comparison of the integrated optical density of detected bands measured by the GIS 1D Gel Image System ver. 3.73 (Tanon, Shanghai, China). The primer sequences are listed in table 1.

### Minigene Construction, Site-Directed Mutagenesis, and Transfection

Genomic DNA isolated from *T. castaneum*, *A. mellifera*, and *B. mori* was taken as template, and PCR was performed to attain the corresponding DNA segments encompassing the alternative spliced exon (but not for *A. mellifera*), the upstream intron, and the upward constitutive exon. Wild-type (WT) minigene DNA was cloned into the pGEM-T Easy vector (Promega). Site-directed mutagenesis was performed on the above gene constructs, having the "AA" changed into "AG" or "AG" changed into "AA," by successive PCR (Aiyar et al. 1996) with an additional pair of mutating primers (table 1). WT and mutant constructs were further cloned into pBluescript-SK+ under the Baculovirus IE1 promoter (a gift from Chenliang Gong, Shuzhou University, China). All constructs were confirmed by sequencing. The linearized DNA was transfected into silkworm cells (BmN) with Lipofectin (Invitrogen) according to the manufacturer's protocol. Total RNAs were harvested 72 h after transfection using Trizol (Invitrogen). RT-PCR and electrophoresis were carried out to detect the splicing status.

The mosquito and fruit fly hybrid minigene containing mosquito exon 3, 5′ conserved part of intron 3 and fruit fly 3′ conserved part of intron 3 and exon 4 was constructed by PCR with primers (table 1). Based on this construct, hybrid minigenes containing a smaller 5′ conserved part of mosquito intron 3 and a smaller 3′ conserved part of fruit fly intron 3 were constructed by PCR with primers (table 1). All constructs were confirmed by sequencing and were transfected into silkworm cells. RT-PCR and electrophoresis were carried out to detect the splicing status. In addition, the spliced variant-specific primers for PCR were designed in a hybrid minigene experiment (table 1). Each splice product was amplified separately from cDNA using a shared forward primer and a reverse variant-specific primer.

### *In Vitro* Transcription

WT or mutant minigenes were placed downstream of the T7 RNA polymerase promoter. Each transcription vector was linearized with *Bst*XI and had ends trimmed with T4 DNA polymerase prior to *in vitro* transcription. Transcription was carried out at 37 °C for 1 h in the following system: linearized DNA 500 ng, 10XT7 RNA polymerase buffer 2 μl, 50 mM dithiothreitol 2 μl, 2.5 mM nucleoside triphosphate mix 4 μl, RNase inhibitor (40 U/μl) 0.5 μl, T7 RNA polymerase (Takara) 10 U, and diethylpyrocarbonate-treated water to 20 μl. The plasmid template DNA was then degraded with 2 U DNase I (Ambion, Austin, TX) after transcription. Synthesized RNAs were collected with Trizol (Invitrogen) and quantified.

**Table 1**
**Primers Used for the RT-PCR and PCR Analysis**

| Primer | Sequence | Primer | Sequence |
|---|---|---|---|
| D/ENK verification and quantification | | | |
| DmeEKVE5′ | AGAGTTTGCCCTACGCCGATG | DmeEKVEq5′ | GGAGTGGCGCGACCTGGTCA |
| DmeEKVE3′ | AGACAATCCGCCCACGTCCATC | DmeEKVEq3′ | CGCAGCGAGAAGCAGATATCT |
| MsD/ENKVE5′ | MGCRATGAACAARACSCTRGTG | MsD/ENKVEq5′ | CGAGAACTGCAGAGCGTCGA |
| MsD/ENKVE3′ | TGAYAAWCCDCCRACRTCCATC | MsD/ENKVEq3′ | CGTAACGCAGCGAGAAGCAG |
| AmeDNKVE5′ | AGCGTACCTTATGCGGATGCG | AmeDNKVEq5′ | AAGCGTCGAGGGTGAAGGTGGT |
| AmeDNKVE3′ | GGATCTGATAAACCACCGACG | AmeDNKVEq3′ | CGAAGCGAGAAGCAAATGTCAC |
| TcaENKVE5′ | AGAACATTCCGTACGCCGATGC | TcaENKVEq5′ | AATGGCGCGAGCTGCAGAGCGT |
| TcaENKVE3′ | AATCCTCCAACGTCCATTTTC | TcaENKVEq3′ | CGTAATGAGAAGCAAATGTCTC |
| BmoDNKVE5′ | TTCAAGAACGTGCCATACGC | BmoDNKVEq5′ | GTGAGCTTCAGAGTGTTGA |
| BmoDNKVE3′ | GAGACCACCGACGTCCATTTTC | BmoDNKVEq3′ | ACGTAACGCAATGAGAAAC |
| PhuENKVE5′ | AATGTTCCGTATGCTGACGC | PhuENKVEq5′ | GAGATTTACAAAGCGTGGA |
| PhuENKVE3′ | TGACAAACCTCCTACATCCAT | PhuENKVEq3′ | ACATAACGTAGCGAAAAGCA |
| DmaENKVE5′ | AGTGCCACTCTGCATGGTCGA | SiGAPDH5′-1 | CTACTGTTCATGCCACAACTGCT |
| DmaENKVE3′ | AGGATGGCCTTACCAATGGGATC | SiGAPDG3′-1 | TGTACTTGATGAGATCAATGACT |
| DroQEK5′ | GGAGTGGAGGGACCTCCA | GgaQEK5′ | GTGACTGAGGAGTGGAGGGA |
| DroQEK3′ | GCAGTTGGCACATACCGCA | GgaQEK3′ | CGGCAGTAGGCACGTAAC |
| VQ verification and quantification | | | |
| DmeVQVE5′ | GATCAAAAAGATCGAGCATG | DmeVQVEq5′ | AGTTGTTGGGATCGGCGTAC |
| DmeVQVE3′ | TTCTGCTCGCTCTGCTTGTCC | DmeVQVEq3′ | TCCTCGGCATTTTCGGTGAG |
| CpiVQVE5′ | AGGGCGAGGCGGAAAAGATC | CpiVQVEq5′ | GGCATGAAAGGAGTCGACCT |
| CpiVQVE3′ | GGACTTTGCCCAGCTTCTGC | CpiVQVEq3′ | CGGTCAGTTCTTCCATGTC |
| AmeVQVE5′ | CTGTAAGCGTAGTAGTTCTC | AmeVQVEq5′ | AACTATTGGGCAGCACGTAC |
| AmeVQVE3′ | ACCTCGCTCTGCTTACTTTC | AmeVQVEq3′ | CTTCGGCATTGTCGGTAAG |
| BmoVQVE5′ | GTGTCGGTGTGGTGATTCTG | BmoVQVEq5′ | AGCTGTTGGGTTCAGCATAC |
| BmoVQVE3′ | GTTTTCCGAGCTTTGTTCC | BmoVQVEq3′ | TCCTCAGCGTTTTCCGTGAG |
| PhuVQVE5′ | ATGCGGATTCTGTATTCGAC | PhuVQVEq5′ | ACAGTTGCTCGGTTCGGCA |
| PhuVQVE3′ | ATCACTCGTTCCTCCCATAT | PhuVQVEq3′ | TCTGCATTTTCCGTTAATTC |
| DpuVQVE5′ | GGACTCAAAGGAGCCGTCGACCT | TcaVQVEq5′ | GTCCAGTTGCTTGGCTCCTC |
| DpuVQVE3′ | CTTGGCCTCGAGGATGACGACAGT | TcaVQVEq3′ | GCATTTTCCGTCAGTTCGTC |
| Mutagenesis | | | |
| AmeDNKWS5′ | CAGGATAACAA***G***TTGGGTGAC | AmeDNKSDM5′ | AATTACAGGA***C***AACAAGTTGGGTGACATTTG |
| AmeDNKWS3′ | TGTCACCCAA***C***TTGTTATCCTG | AmeDNKSDM3′ | CCAACTTGTT***G***TCCTGTAATTAATTTACACC |
| BmoVQSDM5′ | GACTTGCATGTAGGTTCA***A***CC | TcaENKA3′ | GTCACCCAA***C***TTGTTATCCTGTAATATC |
| BmoVQSDM3′ | TATCAGG***T***TGAACCTACATG | AmeENKC3′ | GGGATATCACCTGACCACCTTCACCCT |
| PhuVQSDM5′ | TAGGTTCA***G***CCGGATATGGAAG | TcaENKin5′ | CGACCCCTCCGTTTTTCGAC |
| PhuVQSDM3′ | CTTCCATATCCGG***C***TGAACCTA | DmeVQin5′ | TTTCTAGACGCGCCATTAAATCTTAGT |
| Variant-specific primers | | | |
| AmeDNKSS3′ | GTCACCCAACTGACCAC | CpiDmeVQ3′-3 | TCAGGCTGAACCTTTTCT |
| CpiDmeVQ3′-1 | CCATATCAGGCTTTTCTTTG | CpiDmeVQ3′-4 | TCAGGCTGAACCGATTTTAG |
| CpiDmeVQ3′-2 | CCATATCAGGCGATTTTAGGT | | |

The primers were synthesized to perform site-directed mutagenesis. (The mutated nucleotides were shown in italics.)

*Xenopus* Embryo Microinjection

Microinjection was performed with a HARVARD microinjector according to the operating instructions. Each embryo was injected with 10 nl, and each group consisted of about 30 embryos. Injected embryos were incubated at 18 °C for 1 h before total RNA isolation. RT-PCR and electrophoresis were then carried out to evaluate splicing status.

## Results

### Species-Specific Wobble Splicing is Related to Synonymous Variation in Splice Sites

Two spliced isoforms ($SytI_{VQ}$ and SytI) generated by wobble splicing in *sytI* were previously reported in *A. californica* and were conserved in *Drosophila* and mammalian *sytI* (Nakhost et al. 2003). We subsequently analyzed the nature of alternative splicing in *sytI* orthologs from different insect species. The organisms analyzed were two dipteran species, including *D. melanogaster* (Adams et al. 2000) and one mosquito (*C. pipiens*) (http://flybase.org/blast/), the lepidopteran *B. mori* (Xia et al. 2004; Mita et al. 2004), the coleopteran *T. castaneum* (http://flybase.org/blast/), the hymenopteran *A. mellifera* (Honeybee Genome Sequencing Consortium 2006), and the phthirapteran *P. humanus* (http://flybase.org/blast/). The sequence data from these species allowed us to analyze the evolution of wobble splicing spanning at least 300 My.

Multiple sequence alignment revealed that an AG dinucleotide exists at the intron-distal splice site of the exon only in *D. melanogaster*, *B. mori*, and *A. mellifera*, whereas an AA dinucleotide is present within this site in *T. castaneum*, *C. pipiens*, and *P. humanus* (fig. 1). To validate correlations of this variation with the occurrence of alternative splicing, we designed primers

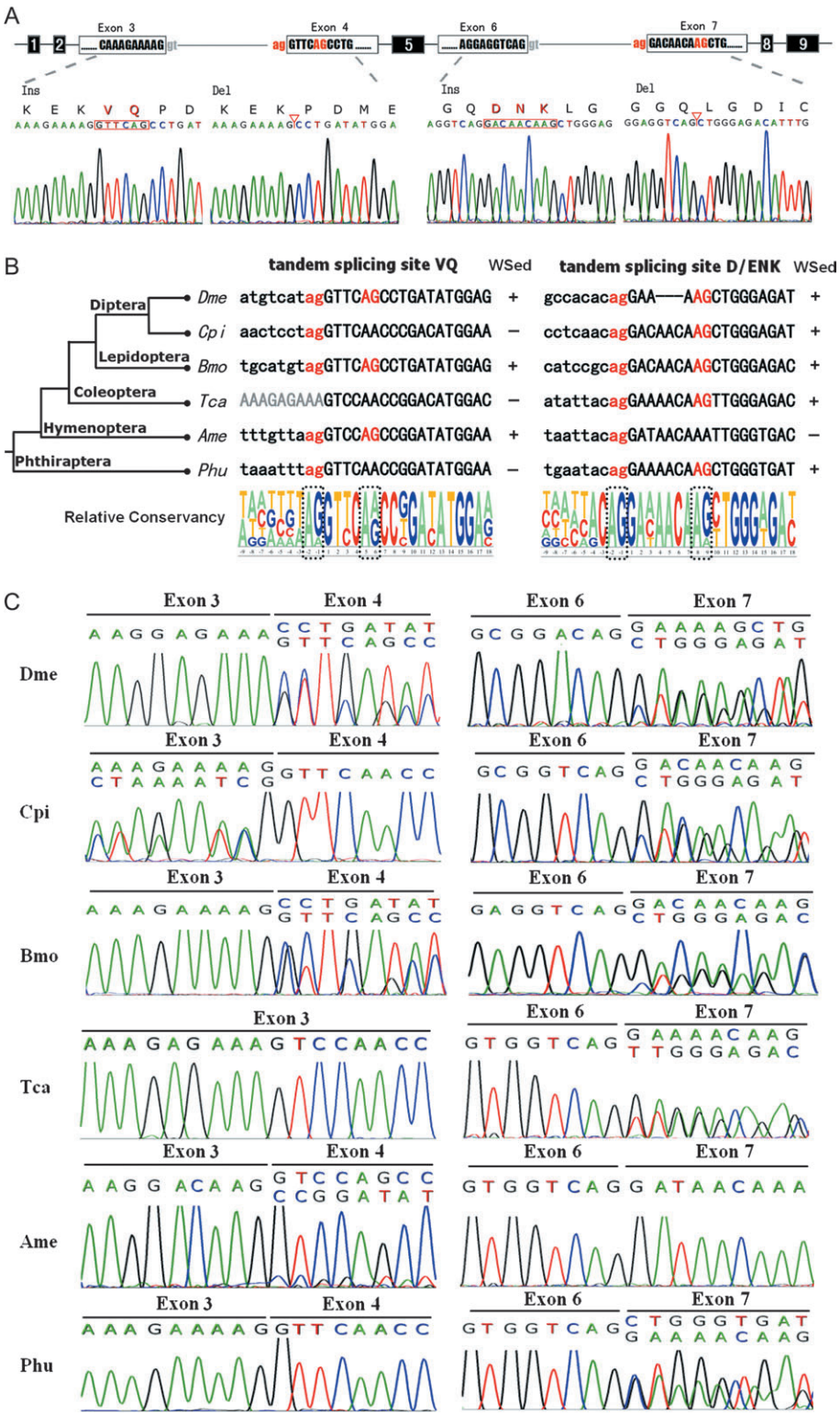


FIG. 1.—Conservation and divergence analysis of wobble splicing in insect *sytI* genes. (*A*). Schematic illustration of insect *sytI* gene structure. Exons are represented by black boxes and the exon–intron architecture is magnified within open boxes. Introns are represented by black lines. "Ins" or "Del" denotes the splicing pattern leading to amino acid insertion or deletion, respectively. Amino acid insertion or deletion is either indicated with red letters or inverted triangles. (*B*). Phylogeny of wobble splicing in insect *sytI* genes from *Drosophila melanogaster* (Dme), *Culex pipiens* (Cpi), *Bombyx mori* (Bmo), *Tribolium castaneum* (Tca), *Apis mellifera* (Ame), and *Pediculus humanus* (Phu). Exonic and intronic sequences are shown in capital and lowercase letters, respectively. The tandem splice sites $[AG(N)_{3n-2}AG]$ diverged during the course of evolution, whereas the distal splice sites were lost in some species. *Tribolium castaneum* was genomically incapable of splicing at this location due to the intron loss. "WSed" denotes "wobble-spliced.". (*C*) Verification of alternative splicing by direct sequencing of RT-PCR products at the former site (VQ) and the latter site [D/E(N)K]. Overlapping nucleotide sequence signals result from wobble splicing.

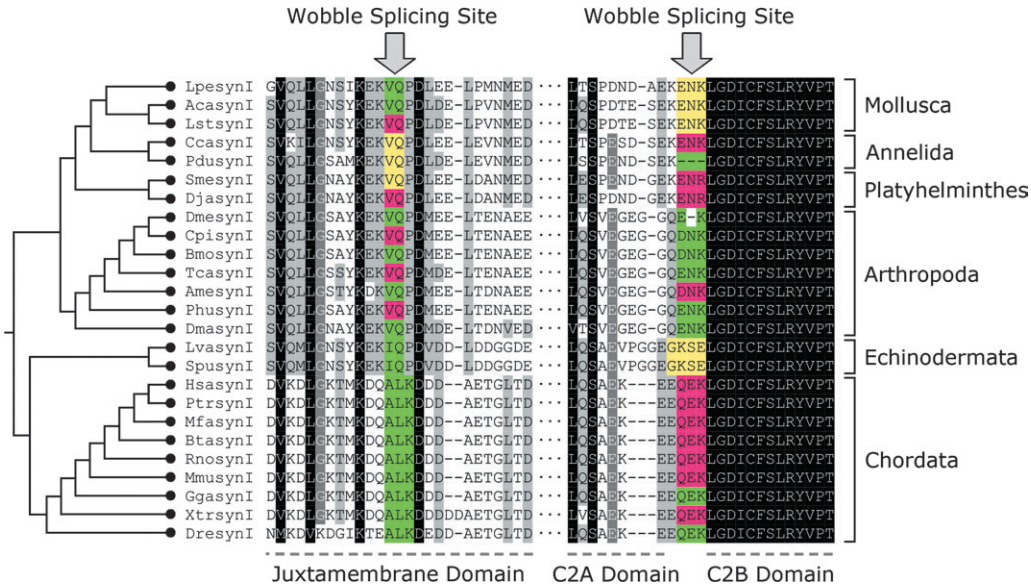


FIG. 2.—Phylogenetic analysis of wobble splicing in metazoan *sytI* genes. Abbreviations: Lpe: *Loligo pealei* (CAA51079.1, BAA09866); Aca: *Aplysia californica* (AAQ91785, P41823); Lst: *Lymnaea stagnalis* (AAO83847); Pdu: *Platynereis dumerilii* (ABR68850.1); Dja: *Dugesia japonica* (BP191518, BP188154); Sme: *Schmidtea mediterranea* (EG350483.1); Cca: *Capitella capitata* (EY537522.1); Dme: *Drosophila melanogaster* (AAF51205); Cpi: *Culex pipiens* (FJ550348); Bmo: *Bombyx mori* (FJ550351); Tca: *Tribolium castaneum* (FJ550350); Ame: *Apis mellifera* (FJ550352); Phu: *Pediculus humanus* (FJ550349); Dma: *Daphnia magna* (FJ550353); Spu: *Strongylocentrotus purpuratus* (AAB67801.3); Lva: *Lytechinus variegatus* (ABA29124.1); Hsa: *Homo sapiens* (BX488459.1, DA206355.1); Ptr: *Pan troglodytes* (DC525743.1, DC521107.1); Mfa: *Macaca Fascicularis* (CJ462565.1, CJ465758.1): Bta: *Bos taurus* (DN522068.1, DV892458.1); Rno: *Rattus norvegicus* (AA924659, CB731032.1); Mmu: *Mus musculus* (NP_033332.1, Q5R4J5.1); Gga: *Gallus gallus* (NP_990502.1, BU141735.1). Xtr: *Xenopus tropicalis* (CX838804, CX839099.1); Dre: *Danio rerio* (CK400350.1, EB976334.1). Phylogenetic tree data were adapted and modified from Dunn et al. (2008). Amino acid residues showing complete conservation are shaded in black. Residues shaded in green were confirmed to be alternatively deleted according to cDNA and EST evidence. Residues in red represent those lacking a tandem splice site. Residues in yellow are those with tandem splice sites without cDNA and EST evidence.

flanking this site in each ortholog. Electrophoresis and sequencing analysis of RT-PCR products were performed to identify alternatively spliced isoforms. As a result, the $SytI_{VQ}$ alternatively spliced form was detected across the SytI orthologs of *D. melanogaster*, *B. mori*, and *A. mellifera*, occurring in a species-dependent manner (fig. 1*C*; supplementary fig. S2*B*, Supplementary Material online). The *A. mellifera* $SytI_{VQ}$ splicing form was much less pronounced than the corresponding form of *D. melanogaster* and *B. mori* (fig. 1*C*; supplementary fig. S2*B*, Supplementary Material online). The wobble splicing occurred in a developmental stage- and tissue-specific manner (supplementary fig. S2*A* and S2*C*, Supplementary Material online). The smaller splicing form was found at a very low level in the larvae but increased during the stages from pupa to adult (supplementary fig. S2*A*, Supplementary Material online). *Tribolium castaneum* was genomically incapable of splicing at this location due to loss of the intron (fig. 1*A* and *B*). We failed to detect alternative splicing at the 3′ acceptor site in *C. pipiens* and *P. humanus*, where the AA instead of the AG sequence is located at orthologous splice junctions (fig. 1*A* and *B*). Alternative splicing at this tandem site is generally conserved in distantly related species (i.e., *D. magna*; *Loligo pealei*; fig. 2), suggesting that $SytI_{VQ}$ should represent the ancestral state in insects. $SytI_{VQ}$ and SytI deviated during the course of insect evolution due to the loss of an intron-distal splice site at the exon 3–4 junction (fig. 1*B*). At the diversion of hymenopteran and phthirapteran orders, an AG dinucleotide was converted into an AA in phthirapterans, whereas an AG remained in the hymenopterans. Similarly, at the diversion of coleopteran and hymenopteran orders, an AG dinucleotide was converted into an AA in the coleopterans, whereas $SytI_{VQ}$ remained in hymenopterans.

A similar situation also occurs in the seventh exon in *sytI*. We discovered that the *B. mori sytI* sequence had a $\Delta 9$ tandem acceptor resulting in an InDel of three amino acids (DNK) prior to the C2B domain (fig. 1). Cross-species alignment of this exon revealed that an AG dinucleotide existed at the intron-distal splice site in all of these species except *A. mellifera*, where an AA dinucleotide was present at this site (fig. 1*B* and *C*). RT-PCR analysis followed by sequencing confirmed that this InDel of three amino acids (DNK) was also conserved across all *sytI* orthologs except for *A. mellifera*, which differed in the ratio of InDels (supplementary fig. S2*B*, Supplementary Material online). Similar to the VQ site, wobble splicing at this site occurred in a developmental stage–specific and tissue-specific manner (supplementary fig. S2*A* and *C*, Supplementary Material online). Moreover, *D. melanogaster* has a tandem acceptor separated by only 6 nt, resulting in the InDel of a dipeptide EK (fig. 1*A*). We detected only one form of spliced transcript in *A. mellifera* embryos, larvae, pupae, and adults (supplementary fig. S2*A*, Supplementary Material online). Similar to previous reports (Tadokoro et al. 2005; Hiller et al. 2006; Unoki et al. 2006; Tsai et al. 2007), these phylogenetic correlations between AG/AA dinucleotide

variations and alternative splicing occurrence indicates that the tandem splice site is necessary for this type of alternative splicing.

## Evolution of Wobble Splicing

SytI proteins are evolutionarily ancient proteins that are conserved throughout the animal kingdom. We analyzed the amino acid sequences of some SytI proteins in Platyhelminthes, Annelida, Mollusca, Arthropoda, Echinodermata, and Chordata. The sequence data from these species allowed us to trace the origin and divergence of wobble splicing. Similar to *A. californica* and *D. melanogaster*, two spliced isoforms ($SytI_{VQ}$ and SytI) generated by wobble splicing were found in squid (fig. 2; supplementary fig. S3, Supplementary Material online). In contrast, only one spliced isoform was found in another molluscan, *L. stagnalis*, where the AA instead of the AG sequence is located at orthologous sites (fig. 2; supplementary fig. S3, Supplementary Material online). Interestingly, alternative splicing at tandem acceptors has also been found in this exact region of the juxtamembrane linker of almost all vertebrate SytI proteins, from low-level fish to high-level mammals, where the amino acids ALK are inserted instead of VQ (fig. 2). Notably, two wobble spliced isoforms ($SytI_{IQ}$ and SytI) have been found in the linker region of SytI in sea urchin (*Strongylocentrotus purpuratus*), which seems to be intermediate between VQ and ALK, consistent with the evolutionary position of the Echinodermata between invertebrates and vertebrates. Intriguingly, a wobble splicing event at this site is generally conserved in Mollusca, Arthropoda, Echinodermata, and Chordata (fig. 2; supplementary fig. S3, Supplementary Material online), indicating that this case is among the few alternative splice events that might have a very deep evolutionary history spanning ~550 My. During evolution, wobble splicing was lost in some species, such as *T. castaneum* and *P. humanus*. In addition, the InDel peptides have diverged into VQ (IQ) and ALK after vertebrate–invertebrate separation.

In contrast to the VQ site, we seldom detected the alternative QEK deletion in the equivalent region of insect D/E(N)K InDel in all vertebrate SytI proteins by Blast-searching against EST databases. As a result, most of these vertebrate *sytI* genes lack the tandem splice site in this region, except for *Gallus gallus* and *Danio rerio* (fig. 2; supplementary fig. S3, Supplementary Material online). The alternative splicing at these tandem splice sites of *D. rerio* and *G. gallus* was confirmed by electrophoresis and sequencing of RT-PCR products (data not shown). In addition, *Schmidtea mediterranea*, *Dugesia japonica*, and *Capitella capitata* (http://genome.jgi-psf.org/euk_cur1.html), which lack the tandem splice site at this site, are thought to generate only one larger spliced isoform, according to EST-based database analyses. However, alternative splicing at this tandem splice site is generally conserved in insect phyla (fig. 2), where an AG dinucleotide represents the ancestral state of this site, at least before the radiation of the coleopteran and hymenopteran orders (spanning ~300 My). At the diversion of coleopteran and hymenopteran orders, an AG dinucleotide was converted into an AA in hymenopterans, whereas an AG remained in place in the coleopterans. Analysis of these orthologs from 12 *Drosophila* species (*D. melanogaster*, *Drosophila simulans*, *Drosophila sechellia*, *Drosophila yakuba*, *Drosophila erecta*, *Drosophila ananassae*, *Drosophila pseudoobscura*, *Drosophila persimilis*, *Drosophila willistoni*, *Drosophila mojavensis*, *Drosophila virilis*, and *Drosophila grimshawi*) (*Drosophila 12 Genomes Consortium 2007*), three mosquitoes (*Anopheles gambiae*, *C. pipiens*, and *Aedes aegypti*) (Holt et al. 2002, http://flybase.org/blast/), and the lepidopteran *B. mori* (Xia et al. 2004; Mita et al. 2004) indicates an AG in these orthologs, whereas AA is also located in *Nasonia vitripennis*, another hymenopteran species (Honeybee Genome Sequencing Consortium 2006; http://flybase.org/blast/). Compared with the former VQ site, wobble splicing at this site is confined to a smaller phyletic branch (fig. 2).

## Wobble Splicing Might be Destroyed by Single Synonymous Variation

Comparative analysis indicates that wobble splicing depends upon whether the 3′ splice junction sequence is AG or AA in insect phyla (fig. 1*B*). It is noteworthy that this AG/AA variation is synonymous but occurs at tandem splice sites. In this way, single synonymous variation could alter wobble splicing. To mimic the natural evolution at tandem acceptors and to investigate their effect on wobble splicing, we introduced a single synonymous change into exon 4 of *B. mori sytI*. Site-directed mutagenesis at the equivalent position to *P. humanus* in the *B. mori sytI* exon 7 was performed, converting the AG into an AA dinucleotide at the 3′ splice junctions (fig. 3*A*). The resulting minigene was evaluated for splicing efficiency and accuracy. As a result, evident wobble splicing of the WT minigene occurred not only in the silkworm cell transfection system but also in the *Xenopus* embryo injection system (fig. 3*B* and *C*), indicating that this construct is clearly sufficient to direct wobble splicing in heterologous splicing systems. However, we only detected one spliced form in the mutated minigene construct in both *in vivo* splicing assays (fig. 3*B* and *C*). Thus, wobble splicing could be abolished through artificial point synonymous substitution in the *sytI* exon. This means that this synonymous variation in *sytI* cannot evolve neutrally but is significantly constrained by splicing requirements.

## Mimicking an Ancestral Tandem Acceptor by Single Synonymous Mutation Fails to Restore Wobble Splicing

To test whether a wobble splicing event can be restored by mimicking an ancestral tandem acceptor, AA-to-AG site-directed mutagenesis was performed at the equivalent position in the *A. mellifera sytI* (fig. 3*A*), which may create a novel 3′ tandem acceptor site like that in *T. castaneum*. WT and mutated minigene constructs encompassing exon 6, the downstream intron, and downstream exon 7, respectively, were prepared based on *A. mellifera* genomic DNA. In transfection experiments on silkworm cells, the mutated minigene could be correctly spliced, but we failed to detect the alternatively spliced form

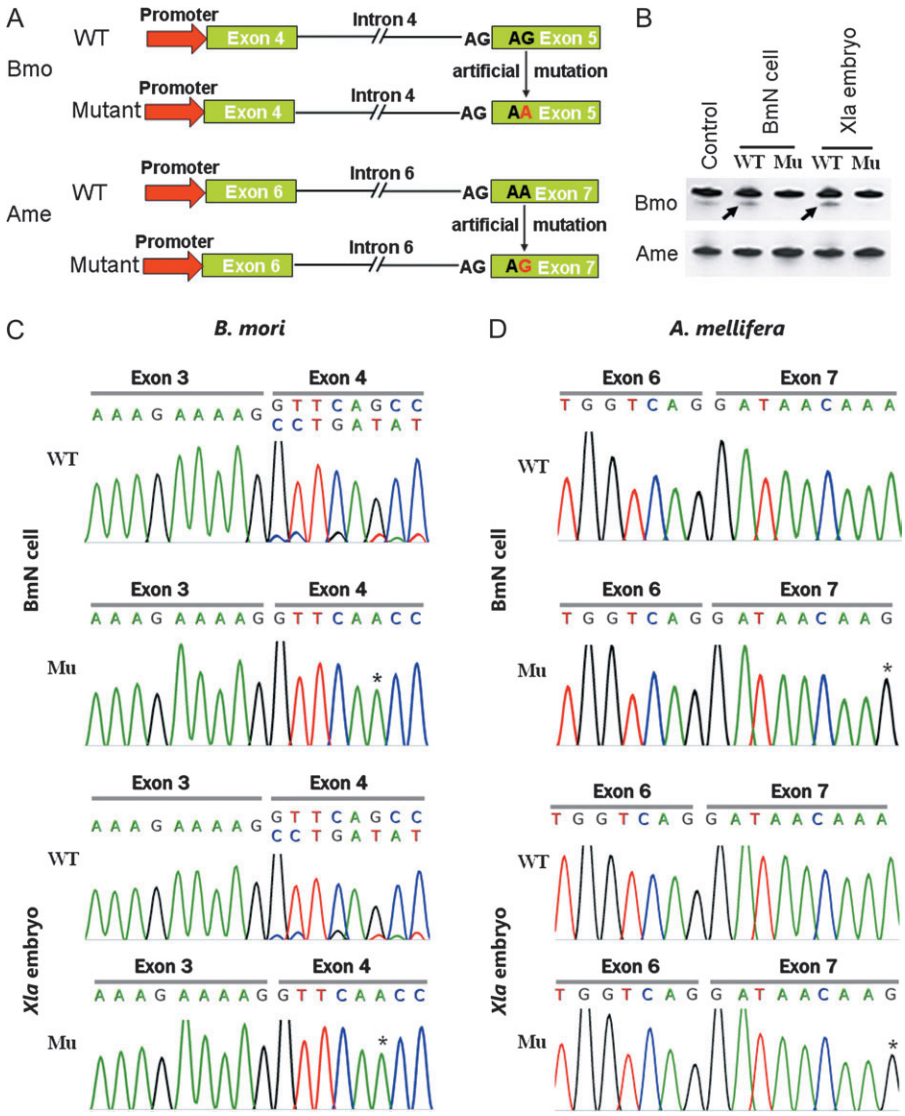


FIG. 3.—Artificial synonymous mutation affects wobble splicing. (*A*) Schematic diagrams of WT and mutant (Mu) minigene constructs involved in *in vivo* splicing assays. T7 and IE1 promoters were used in the *Xenopus* embryo microinjection system and silkworm cell transfection, respectively. Bmo: *Bombyx mori*; Ame: *Apis mellifera*. (*B*) Electrophoresis analysis of splicing profiles. The minigene constructs were introduced into silkworm cells, and splicing profiles were analyzed by electrophoresis in parallel with RT-PCR products. In addition, RNA transcribed with the WT and mutant minigenes by T7 RNA polymerase was subjected to the *Xenopus* embryo microinjection system followed by RT-PCR and electrophoresis analysis. The small spliced forms are marked with arrows. The splicing patterns in *B. mori* and *A. mellifera* embryos were taken as controls ("first lane"). (*C*) Single synonymous variation can destroy wobble splicing. The minigene constructs were introduced into silkworm cells, and the splicing profiles were analyzed by direct sequencing of RT-PCR products. In addition, wobble splicing of WT and mutant minigenes was analyzed in the *Xenopus* embryo microinjection system. The mutated nucleotides are marked with asterisks. (*D*) Mimicking an ancestral tandem acceptor by single synonymous mutation fails to restore *A. mellifera* wobble splicing in *in vivo* splicing assays.

(fig. 3*B* and *D*). We found a similar trend in *in vivo* splicing assays using the *Xenopus* embryo injection system (fig. 3*B* and *D*). In addition, we also failed to detect the alternatively spliced form with a variant-specific primer (data not shown). These results indicate that mimicking an ancestral tandem acceptor fails to restore wobble splicing. Mimicking a tandem acceptor by single synonymous mutation in *P. humanus* also showed similar result. Recognition of the splice sites involves an interaction between the *cis* elements and *trans*-acting factors (Liang et al. 2003). Failure to produce wobble splicing should not be due to a variation of *trans*-acting factors, because wobble splicing of the minigene could occur in both *in vivo* splicing assays (fig. 3*B* and *C*). A recent study indicated that mutations of the region between the branch site and the NAG-NAG 3′ splice site could affect the ratio of the distal–proximal AG selection (Tsai et al. 2007). In addition, a further report indicates that several features of wobble splicing differ from those of constitutive splicing, such as high conservation of the intron sequence upstream of the tandem splice site (Akerman and Mandel-Gutfreund 2006; Koren et al. 2007; Hiller et al. 2008). Moreover, single nucleotide polymorphisms (SNPs) around the NAGNAG motif could affect the splice site choice, which may lead to

a change in wobble splicing pattern (Hiller et al. 2006; Tsai et al. 2007). Finally, a further experiment indicated that the mutation of AA to AG in the *A. mellifera* minigene caused wobble splicing after the *A. mellifera* sequence upstream of the tandem spice site was replaced by that of *T. castaneum*. These data suggest that failure to produce wobble splicing may contribute to a lack of *cis* elements, which are involved in precise recognition of the tandem splice sites. Overall, our evidence from mutagenesis experiments directly demonstrates that the tandem splice

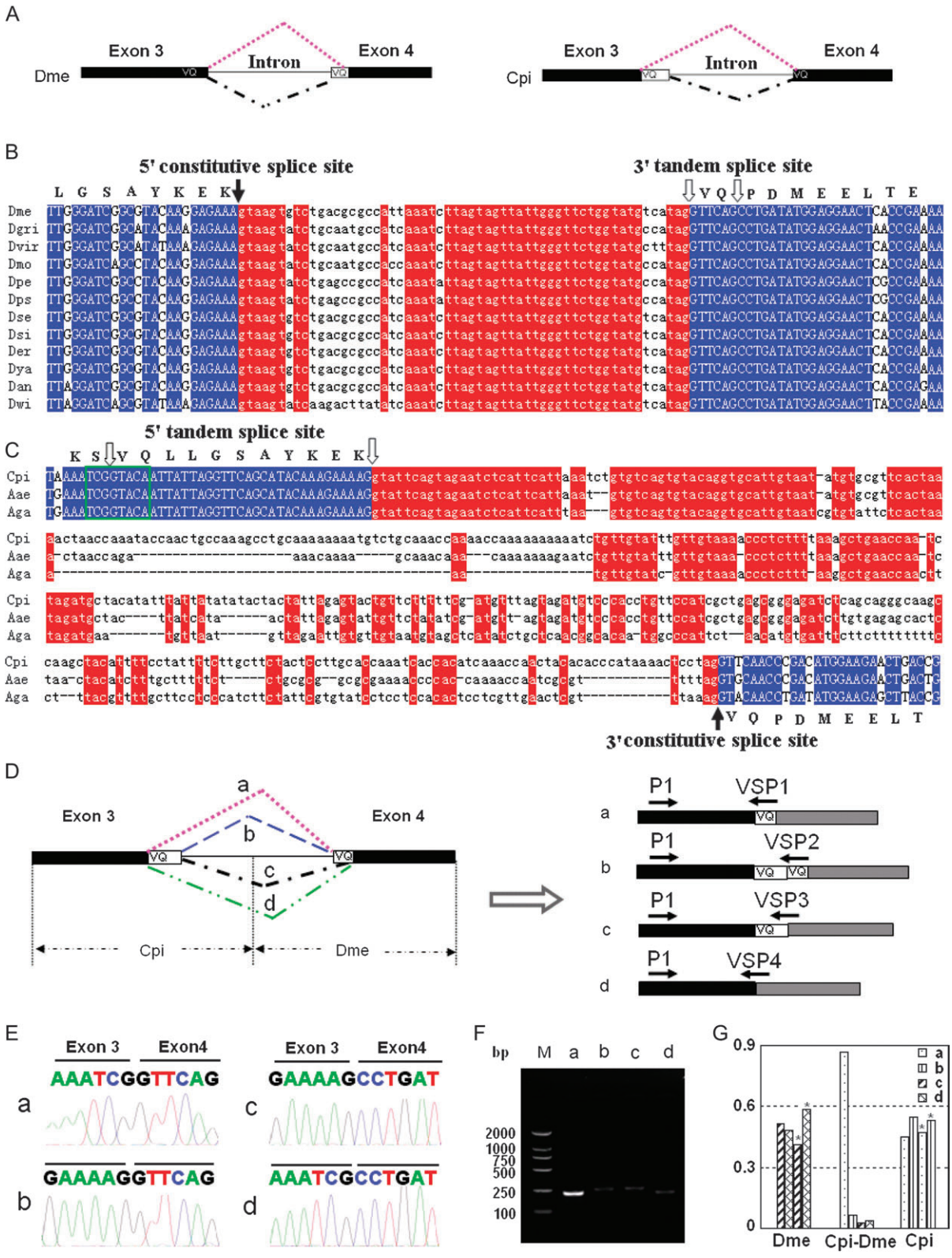

sites are essential, but not alone sufficient, for wobble splicing.

### Alternative Splicing Evolved from 3′ to 5′ Tandem Sites as a Result of an Evolutionary Shift of *cis* Element Sequences

We failed to detect 3′ alternative splicing in exon 4 of *C. pipiens*, whereas AA, instead of AG, is located at orthologous distal 3′ splice junctions. However, we detected alternative splicing at the 5′ tandem donor site in exon 3, resulting in deletion of 11 amino acids (fig. 4*A* and *C*). Interestingly, the first two InDel amino acids are VQ, which are identical to the deleted sequence resulting from 3′ wobble splicing in exon 4 in other species (fig. 4*A*). Thus, the two isoforms, VQ InDel, are caused by alternative splicing at the 3′ tandem acceptor in *D. melanogaster*, *B. mori*, and *A. mellifera*, whereas VQ-like InDel isoforms are generated by alternative splicing at the 5′ tandem donor in *C. pipiens* (fig. 4*A*). Wobble splicing, producing two spliced isoforms with or without VQ, can regulate 5-HT-mediated reversal of depression in *Aplysia* SytI (Nakhost et al. 2003). Considering the similarity of InDel peptides by 5′ and 3′ wobble splicing, it is tantalizing to think that loss of alternative splicing at the 3′ tandem acceptor may be compensated by alternative splicing at the 5′ tandem donor in *C. pipiens*.

Interestingly, *D. melanogaster* also contains a 5′ tandem donor sequence, where TCGGTACA is identical to the distal splice site in mosquito (fig. 4*C*) but fails to undergo alternative splicing. To gauge *cis* elements that may contribute to species-specific alternative splicing, we compared genomic sequences flanking alternative splice sites from 12 *Drosophila* species spanning a ~40-My divergence time (*Drosophila 12 Genomes Consortium 2007*). Sequence alignment revealed invariant intronic and exonic regions in the vicinity of alternative 3′ splice sites (fig. 4*B*), which may contain putative *cis* elements for 3′ tandem acceptor site selection. The remaining intron and exon sequences at the canonical 5′ splice site were relatively divergent. Similarly, genomic sequence alignment from three mosquito species (Holt et al. 2002; http://flybase.org/blast/) also revealed invariant intronic and exonic regions at the 5′ intron–exon boundary (fig. 4*C*), whereas the remaining intronic and exonic sequences at canonical 3′ splice sites were highly divergent. Thus, alternative splicing diverged from 3′ tandem donor to 5′ tandem acceptor in *C. pipiens* after the Drosophilidae–Culicidae separation as a result of an evolutionary shift of *cis* element sequences from 3′ to 5′ splice sites.

To elucidate these conserved elements involved in wobble splicing, we constructed mosquito and fruit fly hybrid minigenes containing *C. pipiens* exon 3, 5′ conserved part of intron 3 and *D. melanogaster* 3′ conserved part of intron 3 and exon 4 (fig. 4*B* and *C*). As a result, sequencing indicated that the 5′ wobble splicing site of the hybrid minigenes was identical to that of mosquito endogenous *sytI* transcripts, whereas the 3′ wobble splicing site was identical to that of fruit fly endogenous transcripts (fig. 4*E*). In addition, each splice variant could be distinguished separately from cDNA using a shared forward primer and a reverse variant-specific primer (fig. 4*D* and *F*). This indicates that the conserved *cis* elements of the hybrid minigene were sufficient to direct wobble splicing at the 5′ and 3′ tandem splice sites. Notably, analysis of expression ratio indicated that this minigene was spliced at a much lower relative splicing ratio at the 5′ intron–proximal tandem donor than the mosquito (fig. 4*G*), suggesting that the fruit fly fragment could affect 5′ tandem acceptor selection and led to predominant usage of the intron-distal 5′ splice site. Conversely, the mosquito fragment also affected 3′ splice site selection of this minigene but led to predominant usage of the intron-proximal 3′ splice site.

## Discussion

### Synonymous Mutation-Mediated Wobble Splicing

Splice acceptors with the genomic NAGNAG motif may cause NAG InDels in transcripts that occur in 30% of human genes and are functional in at least 5% of human genes (Hiller et al. 2004). The intron phase determines the outcome of a NAG InDel and includes single amino acid InDels, exchange of single amino acids, an unrelated dipeptide, or the creation or destruction of a stop codon (Hiller et al. 2004). NAG-to-NAA conversion in phase 0 (synonymous mutation) cannot change the ancestral protein isoform sequence, whereas NAG-to-NAA conversion in phase 1 or

←

FIG. 4.—Comparison of alternative splicing at the 5′ tandem donor in *Culex pipiens* and at the 3′ tandem acceptor in *Drosophila melanogaster*. (*A*) A schematic diagram of wobble splicing in *C. pipiens* (Cpi) and *D. melanogaster* (Dme). Exon sequence is represented by a black box and the alternative sequence (extension) by an empty box. Introns are shown by black lines; alternative splice events are shown by dashed lines; (*B*) Sequence alignment of *sytI* genes from *Drosophila* species. Abbreviations: Dse, *Drosophila sechellia*; Dsi, *Drosophila simulans*; Dya, *Drosophila yakuba*; Dps, *Drosophila pseudoobscura*; Der, *Drosophila erecta*; Dan, *Drosophila ananassae*; Dpe, *Drosophila persimilis*; Dwi, *Drosophila willistoni*; Dgr, *Drosophila grimshawi*; Dvi, *Drosophila virilis*; Dmo, *Drosophila mojavensis*; and Dvi, *Drosophila virili*. Blue and red indicate invariant exon and intron positions, respectively. Alternative and constitutive splice sites are indicated by an empty and black arrow, respectively. (*C*) Sequence alignment of *sytI* genes from *Anopheles* species. Aga: *Anopheles gambiae*; Cpi: *C. pipiens*; and Aae: *Aedes aegypti*. The distal splice site sequences "TCGGTACA" in mosquito, which are identical to that of *D. melanogaster*, are boxed. (*D*) Splicing assay using a hybrid minigene. Mosquito and fruit fly hybrid minigenes contained mosquito exon 3, the 5′ conserved part of intron 3, and fruit fly 3′ conserved part of intron 3 and exon 4. Transient transfection of silkworm cells was performed using a hybrid minigene. The hybrid minigene could give rise to four splice isoforms (*a–d*) by alternative splicing at the 5′ tandem donor and 3′ tandem acceptor. Variant-specific primers (VSP1-4) and shared primers (P1) were designed (table 1) (*E*) Identification of four splice variants by clone sequencing (*a–d*). (*F*) Identification of four splice variants by variant-specific primers. Each splice variant could be distinguished separately from cDNA using a shared forward primer and a reverse variant-specific primer. The products were confirmed to have expected sequences by sequencing. (*G*) The relative occurrence of the four isoforms from the hybrid minigene (Cpi–Dme) was calculated according to sequencing of cDNA clones, and cDNA clones from *C. pipiens* (Cpi) and *D. melanogaster* (Dme) were compared. Sixty to eighty clones were sequenced for every sample. "*" represents the data based on supplementary figure S2, Supplementary Material online.

2 will possibly result in alteration of its amino acid sequence. Thus, NAG-to-NAA conversions in phase 1 or 2 are also constrained by the protein coding sequence, in addition to splicing. This is evidenced by the SNP data in tandem splice sites, where 77% (49 of 64) of SNPs in plausible NAGNAGs are translationally silent but introduce a novel variability at the protein level by changing the acceptor (Hiller et al. 2006). Therefore, wobble splicing in phase 0 is thought to be regulated more compatibly than in phases 1 and 2. Synonymous mutation can convert a tandem acceptor [$AG(N)_{3n-2}AG$] that allows alternative splicing to a nontandem acceptor, $AG(N)_{3n-2}$ AA, that allows only the expression of one transcript. Conversely, conversion of a nontandem acceptor to a tandem acceptor cannot simply mean the occurrence of alternative splicing, which still requires evolutionary coordination of a tandem site and *cis* element sequences.

## Functional Implications

Wobble splicing provides a mechanism to create subtle changes, which may be of functional relevance by changing local hydrophobicity and charge (Hiller et al. 2006). Wobble splicing was detected at two conserved sites in *sytI*. The former has good evidential support for regulating 5-HT-mediated reversal of depression in *Aplysia* (Nakhost et al. 2003), whereas the conservation of the latter splicing event throughout insect evolution points to an important role for this domain. By analyzing the splice site within the context of the 3D structure of the protein domain in which it resides, we are able to propose functional consequences for the InDel of the DNK tripeptide sequence. Homology modeling evidence showed that the three amino acid–DNK tripeptide sequence is just in front of the C2B domain (supplementary fig. S4*A*–*D*, Supplementary Material online). Intriguingly, a comparison between 3D structures of the protein domains of these sequences revealed an extra alpha-helix structure within the C2B domain linker region (supplementary fig. S4*A*–*D*, Supplementary Material online). This subtle structural difference between the two splice isoforms might play an important role for $Ca^{2+}$ binding and conformational change (Garcia et al. 2004). Moreover, regional electron capacity analysis revealed that the linker of the insertion splice isoform showed more hydrophilicity than the deletion isoform linker (supplementary fig. S4*E*, Supplementary Material online). Because the D/E(N)K tripeptide sequence is located within the linker region between C2A and C2B domains, it seems likely that wobble splicing might regulate the precise interactions between C2A and C2B domains, or their binding activity with SNARE, by changing hydrophobicity and charge of the linker.

Interestingly, *sytI* is also a target of A-to-I RNA editing in some insects and squid (Reenan 2005; Yang et al. 2008). In addition, *sytI* also undergoes exon duplication and alternative splicing or other functional wobble splicing in *C. elegans* and *A. californica* (Nakhost et al. 2004; Mathews et al. 2007). These events provide another means to create subtle changes at posttranscriptional stages. Thus, more SytI isoforms are possible through RNA editing and

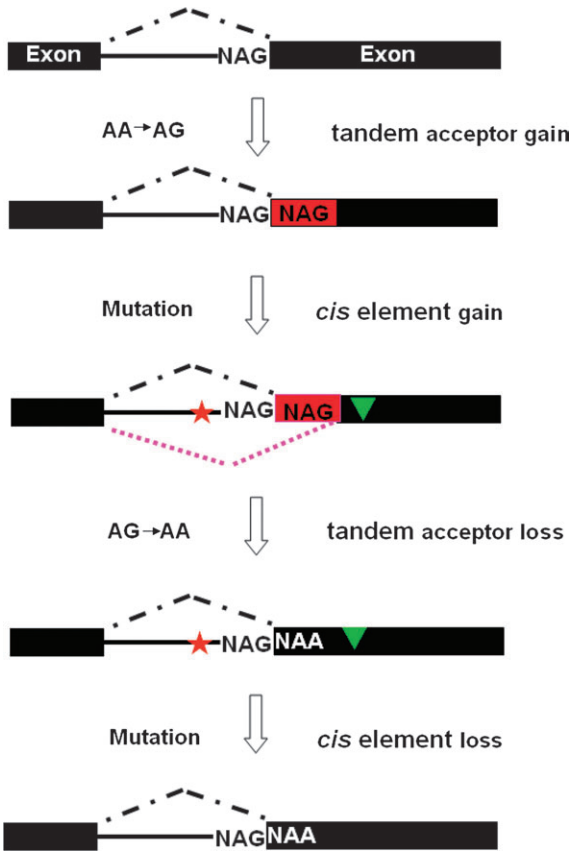


FIG. 5.—An evolutionary model of wobble splicing. The exon sequence is represented by a black box and the alternative sequence (extension) by a red box. Introns are represented by black lines. The ancestral constitutive splice events are shown in black dashed lines, whereas the alternative splice event is shown as a red dashed line. The *cis* elements for wobble splicing are denoted by stars and triangles. The first phase involves the emergence of a novel splice site around an ancestral constitutive exon sequence, for example, by synonymous mutation from A to G that can result in a NAGNAG acceptor. During phase II, the additional *cis* elements were made to be compatible with an intron-distal splice site through nucleotide mutation, which allows alternative splicing. Finally, the functional distal splice site might be destroyed during subsequent evolution, thus resulting in the loss of wobble splicing. Correspondingly, the additional *cis* elements would be degenerated.

alternative splicing, suggesting that there is a general adaptive benefit to managing the regulation of neurotransmitter release in this way.

## An Evolutionary Model of Wobble Splicing

Although these tandem splice sites (i.e., NAGNAG) are common in human genes, only a small subset of sites with this motif is confirmed to be involved in alternative splicing (Liang et al. 2003; Hiller et al. 2004). A recent report indicated that several features of wobble splicing differ from those of constitutive splicing, such as high conservation of the intron sequence upstream of the tandem splice site (Akerman and Mandel-Gutfreund 2006; Koren et al. 2007; Tsai et al. 2007; Hiller et al. 2008). Moreover, evolutionary dynamics of *cis* element sequences also support this view, as evidenced by the shift of *cis* element sequences underlying tandem splice site selection (fig. 4). Our

evidence from mutagenesis experiments directly demonstrates that the tandem splice sites are necessary but not sufficient alone for wobble splicing. These data suggest that the selection of tandem splice sites might not simply be an accident of history but rather in large part the result of evolutionary coadaptation of splice site and *cis* element sequences as a basis for wobble splicing, driven by positive selection. Based on these findings, a plausible evolutionary model for wobble splicing is proposed (fig. 5). The first phase involves the emergence of a novel splice site around an ancestral constitutive exon sequence in the course of evolution, for example, by synonymous mutation from A to G that can result in tandem acceptors. During phase II, the additional *cis* elements produced are compatible with a distal splice site through nucleotide mutation, which allows alternative splicing. The compatibility between splice site and *cis* elements was initially considered to lack biological functionality, but that such functionality was acquired during evolution. The newly created tandem acceptor site might be located within the regulatory range of a *cis*-acting element, and thus alternative splicing occurs immediately after the mutation event, as evidenced by SNP and EST data (Hiller et al. 2006). Alternatively, existing donor or acceptor motifs can function as splice sites if the strength of an adjacent constitutive splice site is reduced by a mutation (Hiller and Platzer 2008). Furthermore, the functional distal splice site might be destroyed during subsequent evolution, thus resulting in the loss of wobble splicing (i.e., *A. mellifera* $SytI_{DNK}$). In addition to neutral mutation, an alternative option to remove a deleterious wobble splicing event might be to destroy the tandem splice site. Correspondingly, the additional *cis* elements are also degenerated. In such a case, wobble splicing fails to occur precisely even if the distal splice site is restored.

## Supplementary Material

Supplementary figures S1–S4 are available at *Molecular Biology and Evolution* online (http://www.mbe.oxfordjournals.org/). Sequence data from this article have been submitted to GenBank (GenBank accession numbers—*C. pipiens*: FJ550348; *B. mori*: FJ550351; *T. castaneum*: FJ550350; *A. mellifera*: FJ550352; *P. humanus*: FJ550349; and *D. magna*: FJ550353).

## Acknowledgments

We acknowledge Julia Hosp for help in commenting on the manuscript. This work was partly supported by research grants from the National Natural Science Foundation of China (90508007, 30770469), and 863 Program (2006AA10A119) and the Program for New Century Excellent Talents in University (NCET-04-0531).

## Literature Cited

Adams MD, Celniker SE, Holt RA, et al. (195 co-authors). 2000. The genome sequence of *Drosophila melanogaster*. Science. 287:2185–2195.

Aiyar A, Xiang Y, Leis J. 1996. Site-directed mutagenesis using overlap extension PCR. Methods Mol Biol. 57: 177–191.

Akerman M, Mandel-Gutfreund Y. 2006. Alternative splicing regulation at tandem 3′ splice sites. Nucleic Acids Res. 34:23–31.

Black DL. 2003. Mechanisms of alternative pre-messenger RNA splicing. Annu Rev Biochem. 72:291–336.

Blencowe BJ. 2006. Alternative splicing: new insights from global analyses. Cell. 126:37–47.

Burgar HR, Burns HD, Elsden JL, Lalioti MD, Heath JK. 2002. Association of the signaling adaptor FRS2 with fibroblast growth factor receptor 1 (Fgfr1) is mediated by alternative splicing of the juxtamembrane domain. J Biol Chem. 277:4018–4023.

Condorelli G, Bueno R, Smith RJ. 1994. Two alternatively spliced forms of the human insulin-like growth factor I receptor have distinct biological activities and internalization kinetics. J Biol Chem. 269:8510–8516.

Craxton M. 2001. Genomic analysis of synaptotagmin genes. Genomics. 77:43–49.

Craxton M. 2004. Synaptotagmin gene content of the sequenced genomes. BMC Genomics. 5:43e.

Drosophila 12 Genomes Consortium. 2007. Evolution of genes and genomes on the *Drosophila* phylogeny. Nature. 450:203–218.

Dunn CW, Hejnol A, Matus DQ, et al. (18 co-authors). 2008. Broad phylogenomic sampling improves resolution of the animal tree of life. Nature. 452:745–749.

Englert C, Vidal M, Maheswaran S, Ge Y, Ezzell RM, Isselbacher KJ, Haber DA. 1995. Truncated WT1 mutants alter the subnuclear localization of the wild-type protein. Proc Natl Acad Sci USA. 92:11960–11964.

Garcia J, Gerber SH, Sugita S, Südhof TC, Rizo J. 2004. A conformational switch in the Piccolo C2A domain regulated by alternative splicing. Nat Struct Mol Biol. 11:45–53.

Geppert M, Goda Y, Hammer RE, Li C, Rosahl TW, Stevens CF, Südhof TC. 1994. Synaptotagmin I: a major $Ca^{2+}$ sensor for transmitter release at a central synapse. Cell. 79:717–727.

Hiller M, Huse K, Szafranski K, Jahn N, Hampe J, Schreiber S, Backofen R, Platzer M. 2006. Single-nucleotide polymorphisms in NAGNAG acceptors are highly predictive for variations of alternative splicing. Am J Hum Genet. 78:291–302.

Hiller M, Huse K, Szafranski K, Jahn N, Hampe J, Schreiber S, Backofen R, Platzer M. 2004. Widespread occurrence of alternative splicing at NAGNAG acceptors contributes to proteome plasticity. Nat Genet. 36:1255–1257.

Hiller M, Platzer M. 2008. Widespread and subtle: alternative splicing at short-distance tandem sites. Trends Genet. 24:246–255.

Hiller M, Szafranski K, Sinha R, Huse K, Nikolajewa S, Rosenstiel P, Schreiber S, Backofen R, Platzer M. 2008. Assessing the fraction of short-distance tandem splice sites under purifying selection. RNA. 14:616–629.

Honeybee Genome Sequencing Consortium. 2006. Insights into social insects from the genome of the honeybee *Apis mellifera*. Nature. 443:931–949.

Holt RA, Subramanian GM, Halpern A, et al. (123 co-authors). 2002. The genome sequence of the malaria mosquito *Anopheles gambiae*. Science. 298:129–149.

Hu CA, Lin WW, Obie C, Valle D. 1999. Molecular enzymology of mammalian Deltal-pyrroline-5-carboxylate synthase. Alternative splice donor utilization generates isoforms with different sensitivity to ornithine inhibition. J Biol Chem. 274:6754–6762.

Joyce-Brady M, Jean JC, Hughey RP. 2001. gamma-Glutamyltransferase and its isoform mediate an endoplasmic reticulum stress response. J Biol Chem. 276:9468–9477.

Koren E, Lev-Maor G, Ast G. 2007. The emergence of alternative 3′ and 5′ splice site exons from constitutive exons. PLoS Comput Biol. 3:e95.

Lai CH, Hu LY, Lin WC. 2006. Single amino-acid InDel variants generated by alternative tandem splice-donor and -acceptor selection. Biochem Biophys Res Commun. 342: 197–205.

Liang XH, Haritan A, Uliel S, Michaeli S. 2003. *trans* and *cis* splicing in trypanosomatids: mechanism, factors, and regulation. Eukaryot Cell. 2:830–840.

Mathews EA, Mullen GP, Crowell JA, Duerr JS, McManus JR, Duke A, Gaskin J, Rand JB. 2007. Differential expression and function of synaptotagmin 1 isoforms in *Caenorhabditis elegans*. Mol Cell Neurosci. 34:642–652.

Maugeri A, van Driel MA, van de Pol DJ, et al. (15 co-authors). 1999. The 2588G→C mutation in the ABCR gene is a mild frequent founder mutation in the Western European population and allows the classification of ABCR mutations in patients with Stargardt disease. Am J Hum Genet. 64: 1024–1035.

Merediz SAK, Schmidt M, Hoppe GJ, Alfken J, Meraro D, Levi BZ, Neubauer A, Wittig B. 2000. Cloning of an interferon regulatory factor 2 isoform with different regulatory ability. Nucleic Acids Res. 28:4219–4224.

Mita K, Kasahara M, Sasaki S. (21 co-authors). 2004. The genome sequence of silkworm, *Bombyx mori*. DNA Res. 11:2 7–35.

Nakhost A, Houeland G, Blandford VE, Castellucci VF, Sossin WS. 2004. Identification and characterization of a novel C2B splice variant of synaptotagmin I. J Neurochem. 89:354–363.

Nakhost A, Houeland G, Castellucci VF, Sossin WS. 2003. Differential regulation of transmitter release by alternatively spliced forms of synaptotagmin I. J Neurosci. 23:6238–6244.

Perin MS, Johnston PA, Ozcelik T, Jahn R, Francke U, Südhof TC. 1991. Structural and functional conservation of synaptotagmin (p65) in *Drosophila* and humans. J Biol Chem. 266:615–622.

Reenan RA. 2005. Molecular determinants and guided evolution of species-specific RNA editing. Nature. 434:409–413.

Tadokoro K, Yamazaki-Inoue M, Tachibana M, et al. (11 co-authors). 2005. Frequent occurrence of protein isoforms with or without a single amino acid residue by subtle alternative splicing: the case of Gln in DRPLA affects subcellular localization of the products. J Hum Genet. 50:382–394.

Tsai KW, Lin WC. 2006. Quantitative analysis of wobble splicing indicates that it is not tissue specific. Genomics. 88:855–864.

Tsai KW, Tarn WY, Lin WC. 2007. Wobble splicing reveals the role of the branch point sequence-to-NAGNAG region in 3′ tandem splice site selection. Mol Cell Biol. 27:5835–5848.

Tsai KW, Tseng HC, Lin WC. 2008. Two wobble-splicing events affect ING4 protein subnuclear localization and degradation. Exp Cell Res. 314:3130–3141.

Unoki M, Shen JC, Zheng ZM, Harris CC. 2006. Novel splice variants of ING4 and their possible roles in regulation of cell growth and motility. J Biol Chem. 281:34677–34686.

Vogan KJ, Underhill DA, Gros P. 1996. An alternative splicing event in the Pax-3 paired domain identifies the linker region as a key determinant of paired domain DNA-binding activity. Mol Cell Biol. 16:6677–6686.

Xia Q, Zhou Z, Lu C, et al. (93 co-authors). 2004. A draft sequence for the genome of the domesticated silkworm (*Bombyx mori*). Science. 306:1937–1940.

Yan M, Wang LC, Hymowitz SG, Schilbach S, Lee J, Goddard A, de Vos AM, Gao WQ, Dixit VM. 2000. Two-amino acid molecular switch in an epithelial morphogen that regulates binding to two distinct receptors. Science. 290:523–527.

Yang Y, Lv J, Gui B, Yin H, Wu X, Zhang Y, Jin Y. 2008. A-to-I RNA editing alters less-conserved residues of highly conserved coding regions: implications for dual functions in evolution. RNA. 14:1516–1525.

Zhang JZ, Davletov BA, Südhof TC, Anderson RG. 1994. Synaptotagmin I is a high affinity receptor for clathrin AP-2: implications for membrane recycling. Cell. 78:751–760.

Michele Vendruscolo, Associate Editor

Accepted January 28, 2009